Electronic Mobilities of Two-Dimensional Transition Metal Dichalcogenides

Thesis

Presented in partial fulfillment of the requirements for the Honors Research Distinction in the College of Engineering of The Ohio State University

Kevin Erik Krymowski

Undergraduate Work in Materials Science and Engineering

The Ohio State University

2015

Thesis Committee

Wolfgang Windl, Sc. D., Advisor

Roberto Myers, Ph. D.

Abstract

In this thesis, two major goals are achieved in regards to studying the electronic mobility of two-dimensional (2D) materials. The first is to establish a method that can reliably predict the electron mobility of planar materials. This was done by applying and adapting an ab-initio calculation method that uses DFT to 2D materials and testing its abilities to reproduce the electron mobilities of well-established 2D materials. We compared the calculated results for the electron mobilities of graphene, graphane, germanane, and single- and multilayered MoS_2 to experiment and find good agreement. After these benchmarks were successful, we extended the method to calculate the hole mobility for the first time. Then we proceeded to predict the electron and hole mobility of 2D WS_2 and WSe_2. We found that WS_2 and WSe_2 have electron (hole) mobilties of 540 (116) and 1424 (435) cm^2/Vs, respectively. These results outperformed the common transition metal dichalcogenides that we performed these calculations on, MoS_2, by a factor of 2 and 6. We go into further analyses, such as looking at the band structures, effective masses, and scattering rates of these materials. We find that the band structures are direct gap at the K point, with WS_2 and WSe_2 having band gaps of 1.98 and 1.61 eV, respectively. The effective electron (hole) masses are 0.39 (0.40) and 0.44 (0.41). We find that the electron velocities give the tungsten TMDs a greater mobility than MoS_2.

Vita

May 2011 ..... Brecksville-Broadview Heights High School

May 2014 ..... B.S. in Material Science and Engineering at OSU

October 2012-Present ..... Undergraduate Research under Dr. Windl

Publications

O. D. Restrepo, K. E. Krymowski, J. E. Goldberger, W. Windl, *A first principles method to simulate electron mobilities in 2D materials*, New J. Phys. **16**, 105009 (2014)

Fields of Study

Major Field: Materials Science and Engineering

Table of Contents

List of Tables

List of Figures

Chapter 1: Introduction

In 2004, Geim and Novoselov produced graphene, a sheet of planar carbon, making two-dimensional (2D) materials a reality[1]. Prior to this event, 2D materials were considered primarily theoretical concepts. Furthermore, graphene was found to have an electron mobility of over 200,000 cm^2/Vs, making is an outstanding conductor. However, it does not have an appreciable band gap, so it is lacking utility as a semiconductor. However, the excitement of the production of graphene and its fantastic electron mobility spurred researchers to investigate graphene and other 2D materials. The main families of materials that are currently being researched are the transition metal dichalcogenides (TMD) and the group IV analogues[2]. However, because these 2D materials are entirely surface, their electronic properties are strongly dependent upon the substrate on which the material lies. This surface dependence makes evaluating these 2D materials problematic. By using modeling simulations to analyze their electronic characteristics in a no strain, vacuum, and known temperature environment, it is possible to properly predict which 2D materials have novel and remarkable properties and are worth practical consideration. 2D materials can be properly modeled by using density functional theory (DFT) and density functional perturbation theory (DFPT). Restrepo *et al.* use the phonon spectra produced from DFT and DFPT to determine the electronic mobility limited by phonons in a process known as lattice scattering.[13] Due to their small

thickness, the phonons in 2D materials are confined, so more care needs to be taken in 2D than in 3D materials to ensure accurate phonon calculations and thus a correct analysis of the lattice-scattering limited mobility in these planar materials. At the same time, adaptions were necessary to the numerics of the code to avoid singularities in 2D which initially either crashed the code or produced non-sensible results. After adapting the methods developed by Restrepo *et al.* for 2D materials, we found good agreement with experiment for well-studied systems. After that benchmarking, we proceeded to identify novel high-mobility 2D transition metal dichalcogenides by predicting their intrinsic maximum mobility, and focused on the electron and hole mobility of 2D WS_2 and WSe_2. We found that WS_2 and WSe_2 have electron (hole) mobilties of 540 (116) and 1424 (435) cm^2/Vs, respectively. These results outperform the abundantly studied transition metal dichalcogenide MoS_2 by a factor of 2 and 6. As our results show, these enhanced mobilities are mostly caused by effective masses.

The following sections are organized as follows: In Chapter 2, A First principles method to simulate Electron Mobilities in 2D Materials is described (which has been published as New J. Phys. **16**, 105009 (2014) and is reproduced here verbatim). In Chapter 3, with the help of Dr. Oscar D. Restrepo and Dr. Wolfgang Windl, a method is developed to determine the hole mobility of 2D materials. We calculate the electron and hole mobility of two tungsten dichalcogenides, WS_2 and WSe_2 and explain the differences in their electron mobility relative to MoS_2. Finally in Chapter 4, the conclusions from Chapters 2 and 3 are summarized.

Chapter 2: A First principles method to simulate Electron Mobilities in 2D Materials

[Published as New J. Phys. **16**, 105009 (2014)]

Oscar D. Restrepo[1], *Kevin E. Krymowski*[1], *Joshua Goldberger*[2], *and Wolfgang Windl*[1]

1. Department of Material Science and Engineering, The Ohio State University, Columbus OH 43210

2. Department of Chemistry and Biochemistry, The Ohio State University, Columbus OH 43210

Abstract

We examine the predictive capabilities of first-principles theoretical methods to calculate the phonon- and impurity limited electron mobilities for a number of technologically relevant two-dimensional materials in comparison to experiment. The studied systems include perfect graphene, graphane, germanane and MoS_2, as well as graphene with vacancies, and hydrogen, gold, and platinum adsorbates. We find good agreement with experiment for the mobilities of graphene (μ = 2x10^5 cm^2/Vs) and graphane (μ = 166 cm^2/Vs) at room temperature. For monolayer MoS_2 we obtain μ = 225 cm^2/Vs. This value is higher than what is observed experimentally (0.5-200 cm^2/Vs) but is on the same order of magnitude than other recent theoretical results. For bulk MoS_2 we obtain μ=48

cm^2/Vs. We obtain a very high mobility of 18,200 cm^2/Vs for single-layer germanane. The calculated reduction in mobility from the different impurities compares well to measurements where experimental data are available, demonstrating that the proposed method has good predictive capabilities and can be very useful for validation and materials design.

Introduction

Ever since the advent of graphene,[1] the effort has greatly intensified to discover new kinds of two-dimensional (2D) materials with intrinsic properties that will make them ideal for electronic applications.[2] Of special interest are their transport properties, in particular their electronic mobilities that for example in suspended graphene can reach hundreds of thousands cm^2/V-s, although external influences such as substrates, impurities, and contacts make it hard to reach that limit.[3] These prospects have not only triggered considerable effort in the research of non-graphene 2D material, but have moved the question for their ideal electronic and transport properties, as well as their potential to perform at or close to their theoretical limit, in a central position. For that, a well-validated, parameter-free method that can predict the limiting carrier mobilities for the ideal material, as well as the effect of external influences, would be highly desirable in order to assess the real-life usability of novel and existing 2D materials, decide how much a certain device structure, contact or substrate influences their "natural" conductivity, as well as explore and design novel materials that have specific desired properties. In this paper, we discuss such a method that has been recently proposed to be applicable to 2D materials for germanane,[4] a germanium-based graphane analogue, and apply it to a number of other 2D test systems, including graphene without and with impurities, graphane, and MoS_2 (single-layer and bulk limits), for which we examine its predictive powers in light of the available experimental results. The good predictive capabilities of this method that we find, in combination with the fact that no idealized or ad-hoc materials properties have to be used as is common in most all other methods,

opens the prospect of targeted 2D design, as well as providing a tool that allows (indirect) structure validation from the transport and optical properties in cases where direct imaging of the synthesized 2D material is difficult.

Theoretical Method

Mobility is a key quantity in electronic transport since it describes how the motion of a charge carrier is affected by an applied bias. Conventional mobility models usually suppress atomic-scale detail when treating two-dimensional or thin-layer semiconductor systems, using effective mass theory[5] or bulk energy bands to calculate the kinetic energy of electrons.[6] After that, also the main scattering mechanisms that limit mobilities, which are due to phonons and ionized impurities,[7] are often treated in an approximate way. Until recently, calculations of electron-phonon scattering rates have relied on empirical deformation potentials and rigid pseudo-ion models.[8,9,10] Large differences among empirical deformation potentials have been found in the literature,[11] and only recent theoretical advances start to produce deformation potentials calculated with first-principles methods that may clarify this situation.[12] A comparison of several numerical approaches to calculate electron-phonon scattering rates at high energies reported in Ref. [9] illustrates the complexity of the problem.

With the emergence of two-dimensional materials that consist only of surfaces and thus show strong effects from environmental effects and adsorbates, predictive parameter-free theoretical methods for the calculation of carrier mobilities that take into account

quantum mechanical effects at the atomic level have become a necessity. Here, we apply a first-principles method that we have developed in the past for 3D semiconductor materials to calculate mobilities limited by phonon and ionized impurity scattering to a selection of 2D materials.[13] We will refer to this approach in the following as the Ab-Initio Mobility (AIM) method.

Our approach is based on the linearized Boltzmann equation in the relaxation time approximation. Ground state calculations were performed within the Quantum ESPRESSO[14] software package using the local density approximation (LDA)[15] for exchange and correlation functionals unless otherwise indicated. Several key quantities such as wave functions, eigenenergies and electron-phonon coupling constants are extracted from this package. To calculate the mobility we use[16]

$$\mu = -\frac{2e}{n_c}\sum\int_0^{k_F}\frac{d^3\vec{k}}{(2\pi)^3}\tau(\vec{kj})\vec{\upsilon}_j^2(\vec{k})\frac{\partial f}{\partial \varepsilon}\bigg|_{\varepsilon=\varepsilon_{nk}}, \qquad (1)$$

where n_c is the density of carriers, $\tau(\vec{kj})$ is the momentum relaxation time for electrons in state $(\vec{kj})$, $\vec{\upsilon}_j(\vec{k})$ their group velocity, and f the Fermi-Dirac distribution.

In order to determine $\tau(\vec{kj})$ for the case of scattering of electrons due to phonons, we use Fermi's Golden Rule,

$$\frac{1}{\tau(\vec{k}j)} = \frac{2\pi}{\hbar}\sum_{\vec{q}\lambda j'}\left|g^{\vec{q}\lambda}_{\vec{k}+\vec{q}j',\vec{k}j}\right|^2 \left\{\left[\, f(\varepsilon_{\vec{k}+\vec{q}j'}) + n_{\vec{q}\lambda}\,\right]\right.$$
$$\cdot\delta(\varepsilon_{\vec{k}j} - \varepsilon_{\vec{k}+\vec{q}j'} + \hbar\omega_{\vec{q}\lambda}) + \left[1 + n_{\vec{q}\lambda} - f(\varepsilon_{\vec{k}+\vec{q}j'})\right] \qquad (2)$$
$$\left.\cdot\delta(\varepsilon_{\vec{k}j} - \varepsilon_{\vec{k}+\vec{q}j'} - \hbar\omega_{\vec{q}\lambda})\right\}$$

where g is the electron-phonon coupling function, $f(\varepsilon_{\vec{k}+\vec{q}j'})$ are the Fermi-Dirac occupation factors, $\varepsilon_{\vec{k}j}$ the band energies, $\omega_{\vec{q}\lambda}$ the phonon frequencies, and $n_{\vec{q}\lambda}$ is the Bose-Einstein distribution function. The derivation of Eq. 2 (see [16]) considers both scattering of an electron from state k to k+q and also backscattering from k+q to k by either emission or absorption of phonons. The electron-phonon coupling matrix element g is given by

$$g^{\vec{q}\lambda}_{\vec{k}+\vec{q}j',\vec{k}j} = \sqrt{\frac{\hbar}{2M\omega_{\vec{q}\lambda}}}\left\langle \Psi_{\vec{k}+\vec{q}j} \left| \frac{dV_{e-p}}{du_{\vec{q}\lambda}}\cdot e_{\vec{q}\lambda} \right| \Psi_{\vec{k}j} \right\rangle, \qquad (3)$$

where M is the atom mass, $e_{\vec{q}\lambda}$ are phonon polarization vectors, $u_{\vec{q}\lambda}$ represent atom displacements with periodicity $\vec{q}$, relative to their equilibrium positions, $\vec{R}$ and V_{e-p} is the screened one-electron potential. The interatomic force constants and phonon frequencies are determined by density functional perturbation theory,[17] as implemented in the Quantum Espresso package. The normalization with respect to the number of ions is already included in the wave functions and thus does not appear explicitly in Eq. (3). Ab-initio calculations of spectral functions $\alpha^2F(\omega)$, which are directly proportional to the electron-phonon coupling g, compare well with experiment,[17] providing a direct test of

the validity of the calculated *g* and indirectly of the accuracy of the Kohn-Sham orbitals used in these calculations.

The Coulomb scattering rate for impurities and defects is calculated as[16]

$$\frac{1}{\tau(\vec{k}j)} = \frac{2\pi n_d}{\hbar}\sum_{j'}\frac{V}{(2\pi)^3}\int d^3\vec{k}'\delta(\varepsilon_{\vec{k}j}-\varepsilon_{\vec{k}'j'}) \times\left|T_{j',j}(\vec{k}',\vec{k})\right|^2(1-\cos\theta), \qquad (4)$$

where V is the volume of the macrocrystal, and θ is the angle between $\vec{\upsilon}_j(\vec{k})$ and $\vec{\upsilon}_{j'}(\vec{k}')$. Within the Born approximation, the scattering matrix $T_{j',j}(\vec{k}',\vec{k})$ is given by $T_{j',j}(\vec{k}',\vec{k}) = \left\langle \vec{k}j\left|\Delta V\right|\vec{k}'j'\right\rangle$ where the self-consistent scattering potential $\Delta V = V_{\text{def}} - V_{\text{ref}}$ is the difference between the potential of a reference "unperturbed" system and the potential of the system in the presence of a defect or impurity. We have included screening of the scattering potential as described in [13] in the Debye parameterization, where the screening length is proportional to the inverse square root of the electronic density. All the integrals over k-space have been evaluated using the tetrahedron method.[18]

The method used here has been applied successfully to bulk semiconductors in the past, where good agreement was found for the case of silicon [13] (the room temperature phonon-limited electronic mobility was calculated to be 1900 cm^2/Vs vs. an experimental value of 1500 cm^2/Vs) and also for diamond [19] (the calculated value is 130 cm^2/Vs while the experimental value[20] is between 100 and 660 cm^2/Vs, with more recent values closer to the lower end). Also, a very recent adaption of our method by others[21] and

expansion to use Monte Carlo transport simulations instead of the relaxation time approximation for MoS_2 give results very similar to ours as discussed below, supporting the use of the computationally much easier and more efficient relaxation time approximation used here.

Results and Discussion

In this paper, we will examine a series of materials which are currently widely studied, but for which either accepted experimental mobilities have been established or for which questions exist that require theoretical calculations that are not based on experimental parameters. These include the "suspended" mobility limit in graphene, graphane, and in MoS_2, the question if the electron mobility in single-layer MoS_2 beats that of bulk MoS_2, and how a full quantum-mechanical treatment of the effect of impurities on the mobility compares with available experiments.

Due to this high environmental sensitivity of 2D materials and the difficulty in ensuring and monitoring the material and its surroundings, a full exploration of the electronic properties of a wider range of 2D materials under full control of geometric and environmental conditions is currently only possible from the theoretical side, i.e. by calculation. Since these calculations do not include any free parameters, they can be used to predict the potential of new 2D materials for the optimization of future electronic devices. Our results are summarized in Table I in comparison to experiment and will be discussed in detail in the following.

Table I: Calculated phonon and impurity limited mobility compared with experiment

	Phonon-limited Mobility (cm^2/Vs)	
	Calculated	**Experiment**
Graphene	$2x10^5$	$1.2x10^4$
Graphane	166	150
Germanane	18195	
MoS2 (monolayer)	225	0.5-200
MoS2 (bulk)	47.9	15
	Impurity-limited Graphene Mobility at $N=10^{12}$ defects	
Au adatom	3169	2801
Pt adatom	150198	409514
Vacancy	950	
Hydrogen	34295	

(a) Suspended Graphene and Graphane

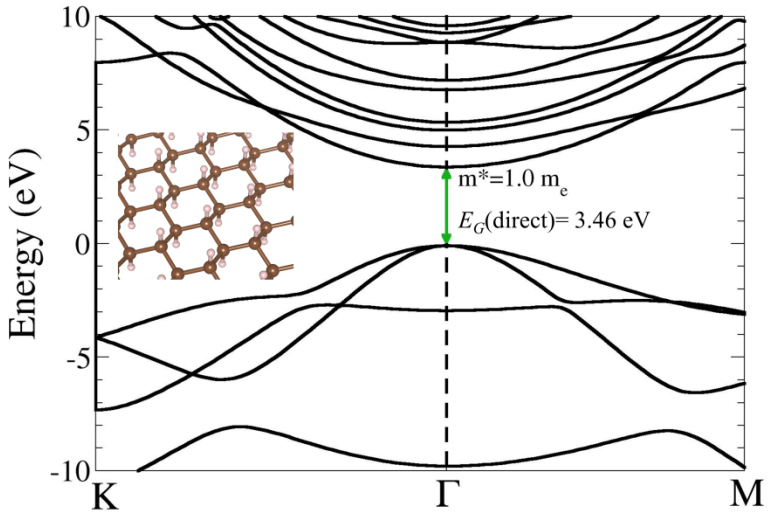

Figure 1: Graphane band structure, calculated within PBE.

Since the zero-band gap of graphene limits its use to applications that do not require a band gap, hydrogenated graphene[22] (graphane, Fig. 1) has recently received more attention, which is a semiconductor with a theoretical band gap of 5.4 eV.[23] This material has also attracted a lot of interest for its possible applications in hydrogen storage. The measured electron mobility of 150 cm^2/V-s for graphane on a SiO_2/Si substrate[24] is several orders of magnitude lower than that of graphene, and to date it is not clear if graphane suffers from similarly detrimental effects of the substrate on the carrier mobility as graphene does, where suspended graphene has a conductivity that is at least 1-2 orders of magnitude larger than that for graphene on a substrate. However, since one may expect that hydrogen "protects" the in-plane carbon bonds better from substrate effects than is

the case in graphene, it would be conceivable that graphane is closer to its theoretical limit than graphene, which we will investigate here.

For single-layer graphene we obtain a mobility of 200,000 cm^2/Vs. This is in reasonable agreement with mobility measurements of free-standing graphene (up to 120,000 cm^2/V-s) and with previous predictions.[24,25] Thinking in terms of effective masses, this is consistent with the fact that the carrier mass in the Dirac cone around the pseudo-gap is very small with a value of 0.012 free electron masses (m_e).[26]

However, this situation is very different for graphane. There, we obtain a PBE[27] direct band gap at the Γ point of 3.46 eV and a conduction effective mass of 1 m_e (Fig. 1). Due to the fact that PBE underestimates band gap values, as has been shown for graphene previously where the hybrid HSE06 functional finds a value of 5.4 eV,[23] we don't expect a perfect agreement with experiments for the band gap. On the other hand, effective masses are usually well reproduced by traditional DFT. The relatively high effective mass in graphane thus indicates a much lower electron mobility than in graphene, which is indeed the case. We calculate for perfect, suspended graphane an electron mobility of 166 cm^2/Vs. This is in excellent agreement with the experimental value of 150 cm^2/Vs [[28]], which is little disputed. Thus, we find for perfect 2D carbon films sensible results within the AIM approach, which especially predicts that substrates have a small to negligible effects on the electron mobility in graphane, in contrast to graphene.

(b) Graphene with Adsorbed Impurities: Importance of Screening

To further compare with experiments, we have performed impurity-limited graphene mobility calculations for platinum and gold adatoms, for which experimental values are available [29,30]. Au and Pt adatoms both have their minimum-energy position in the center of a graphene ring, 2.37 and 1.82 Å above the graphene plane, respectively. In addition, we also examine vacancies as well as dilute hydrogen passivating the p_z orbital of a C atom, in order to examine the effect of point defects as well as the mobility in slightly hydrogenated graphene.

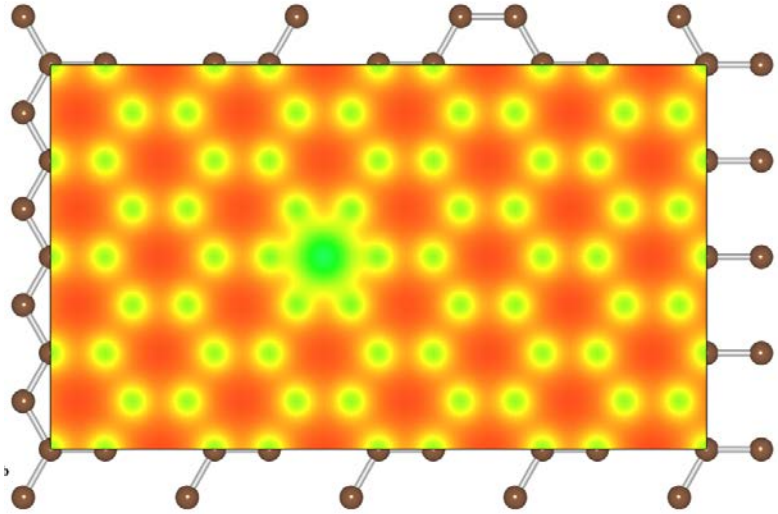

Figure 2: Self-consistent electronic charge density of a graphene monolayer with an Au ad-atom left of the center.

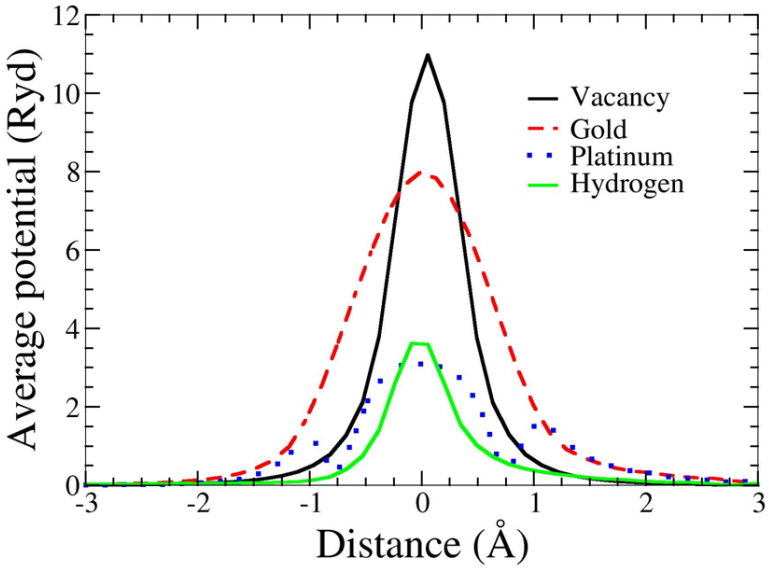

Figure 3: Self-consistent scattering potentials for different impurities in graphene as labeled. Au and Pt are adatoms, while H passivates the C pz orbitals.

The typical changes in the electronic charge density when adding an impurity – here Au – are shown in Fig. 2. Figure 3 shows the radially averaged scattering potentials generated by them. The vacancy and the Au-adatom potentials have the greatest impact on scattering while the potentials for Pt adatoms and hydrogenated C atoms are about half as large. As shown in Figs. 4-5 in the case of Au and Pt adatom impurities, we find that inclusion of screening leads to a much better agreement with available experimental data from McCreary et al. [29] and Pi et al. [30], respectively. At 10^{12} defects per cm^2, we obtain mobilities of 3,200 (Fig. 4), 150,200 (Fig. 5), 950 (Fig. 6), and 34,300 (Fig. 7) cm^2/Vs for Au, Pt, vacancies and H impurities, respectively. As expected, the larger

mobilities are given by the smaller potentials (Pt and H) while the smaller mobilities correspond to the larger potentials of Au and vacancies. These calculations represent the first fully quantum mechanical and parameter free predictions of mobilities from impurity, and demonstrate in comparison to experiment the significant influence of screening on the mobility.

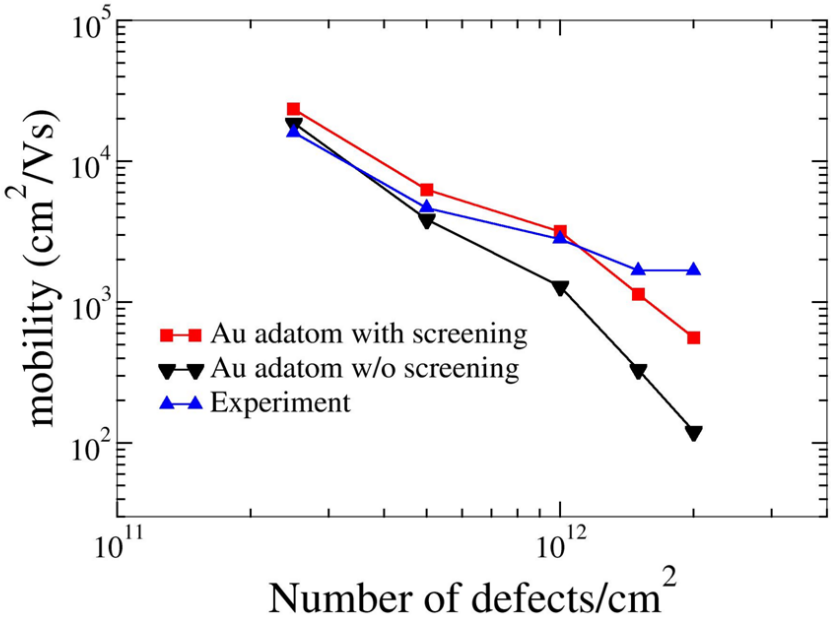

Figure 4: Electron mobility due to impurity scattering as a function of Au adatom concentration on graphene compared with experiment [29] (T = 18 K).

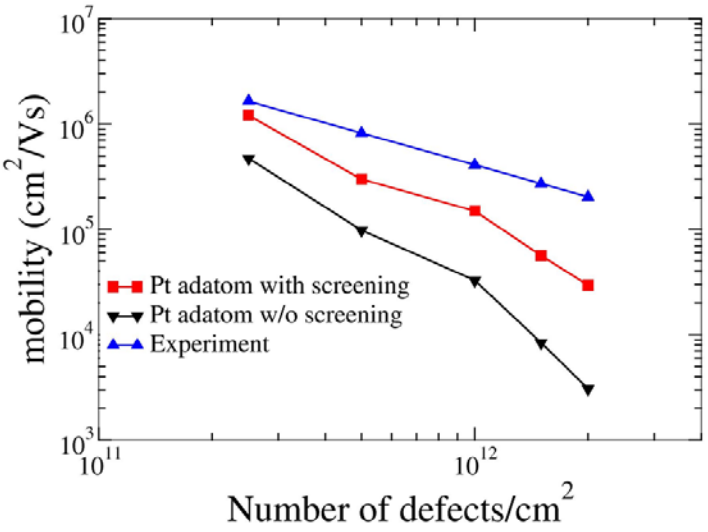

Figure 5: Electron mobility due to impurity scattering as a function of number of Pt adatom concentration on graphene compared with experiment [30] (T = 18 K).

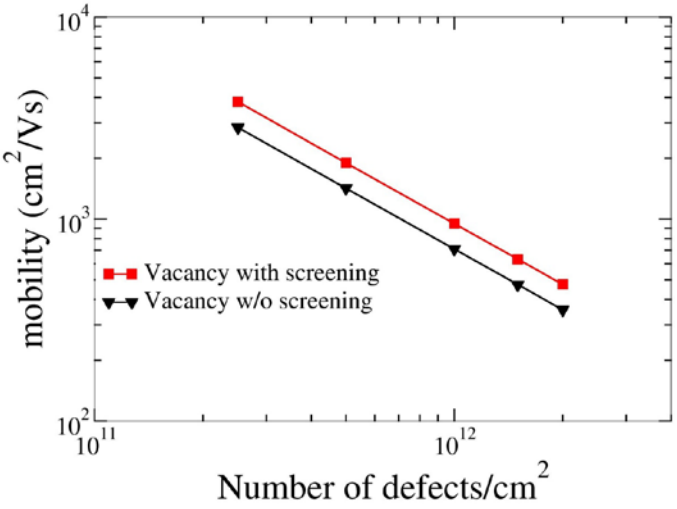

Figure 6: Electron mobility due to impurity scattering as a function of vacancy concentration in graphene (T = 18 K)

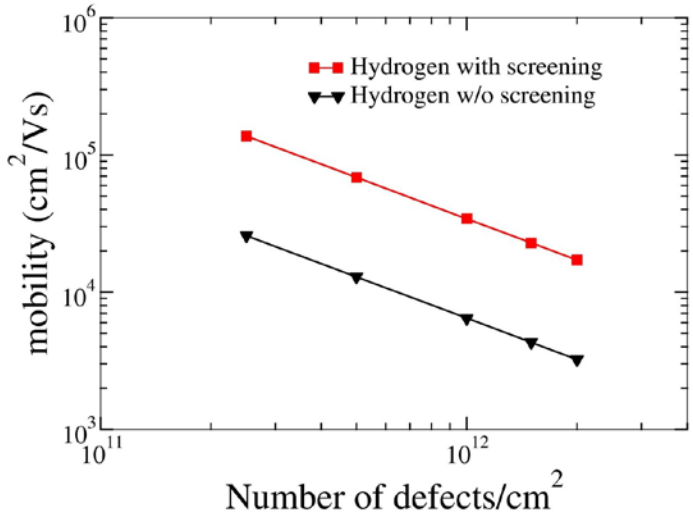

Figure 7: Electron mobility due to hydrogen impurity scattering as a function of number of defects (T=18K)

(c) Novel non-carbon materials: MoS_2 and germanane

Among the newly discovered 2D materials, single-layer (SL) MoS_2 has been of particular interest due to its intrinsic band gap, which enables using it in conventional transistor structures for electronic switching, and the suggested prospect of enhancing its air-based carrier mobility, proposed to be in the single-digit numbers, to ~200 cm^2/V-s by dielectric engineering, e.g. within a HfO_2/SL-MoS_2/SiO_2 structure.[31] However, an alternative explanation may be that the latter measurement simply involved a structure and SL-MoS_2 material that allowed electron conduction closer to the "perfect" limit, which we will

examine within the current work. Also, the suggested use of multi-layer instead of SL MoS_2 to facilitate device fabrication[31] has opened up the question for a more detailed study of the mobility of the multi-layer limit, i.e. bulk MoS_2, where the SL-MoS_2 sheets are held together by van der Waals forces.

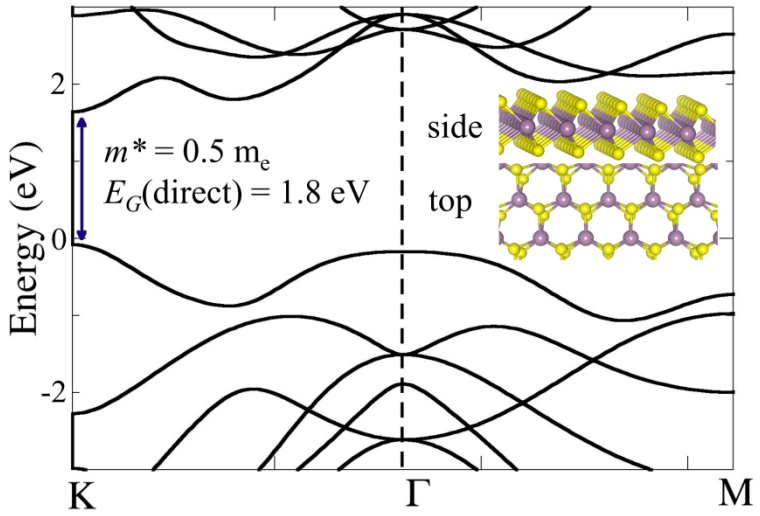

Figure 8: Monolayer MoS_2 band structure, calculated within PBE.

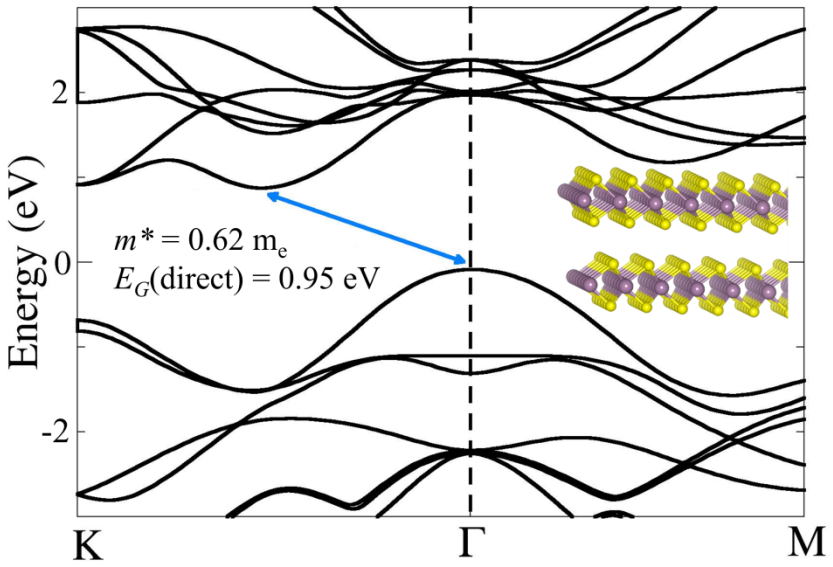

Figure 9: Bulk MoS_2 band structure, calculated within PBE.

The MoS_2 monolayer has a PBE direct band gap of 1.8 eV and a conduction effective mass of 0.5 (Fig. 8). Bulk MoS_2 has an indirect PBE band gap of 0.95 eV and a conduction effective mass of 0.62 (Fig. 9), which is in good agreement with previous theoretical simulations.[32] For single layer MoS_2 the experimental mobility values ranges from 0.5-3 cm^2/Vs in recent studies,[33,34] much lower than the originally measured values of 100-260 obtained by Fivaz et al.[35] More recently a value of 200 cm^2/Vs was achieved by Radisavljev et al.[31] Our calculated value of 225 cm^2/Vs gives a very reasonable upper bound to these measurements, while the sensitivity to external effects that we demonstrated for graphene may explain why also much lower values over a wide range have been measured. Other very recent theoretical efforts have found values for single-layer MoS_2 of 130 cm^2/Vs (potentially up to 320 cm^2/Vs due to numerical uncertainties)

[36] by using a combination of density functional calculation with Monte Carlo simulations and a value of 410 cm^2/Vs [37] by using first-principles to obtain acoustic and optical deformation potentials and the Fröhlich interaction, both in the same range as our result, but most possibly with larger uncertainties and computational efforts. For bulk MoS_2 we obtain an electronic mobility of 48 cm^2/Vs which is higher than the experimentally reported mobility of 15 cm^2/Vs. [38]

Very recently, another type of 2D semiconductor named germanane has been realized, where [111] sheets of bulk germanium are terminated by varying functional groups such as H [4] or CH_3 [39]. Of these two we studied hydrogenated germanane (GeH), where we obtain a direct band gap of 1.56 eV at the Γ point for an isolated layer using the hybrid HSE06 exchange-correlation function, [40,41,42] which typically calculates band gaps in close agreement with experiment, which in the case of germanane finds a value of 1.59 eV [4]. The calculated effective mass at the conduction band at Γ is 0.09 m_e. This low effective mass leads to a high mobility of 18,200 cm^2/Vs for single-layer germanane,[4] making it probably the (non-zero band-gap) semiconductor with the highest electron mobility.

Conclusions

In this work, we have used first-principles methods to calculate the electron mobilities for the technologically relevant two-dimensional materials graphene, graphane, MoS_2, and germanane. Our phonon-limited results for graphene, graphane and single-layer MoS_2 compare favorably with experiments. We find that graphane seems to be much more

insensitive to substrates than graphene, which we rationalize by the protecting effect of the H-atoms on the conducting C-layer. For bulk MoS_2 the theoretical value (48 cm^2/Vs) is about three times larger than the measured one, but is still considerably smaller than the SL value. Our findings for single-layer MoS_2 are supported by other recent theoretical results that give values of the same order of magnitude as reported here, but should be computationally more efficient and thus wider applicable. Finally, AIM predicts a mobility of 18,200 cm^2/Vs for the recently synthesized germanane, which thus would be the fastest of all semiconductors with non-zero band gap.

We further investigated the effect of impurities on the electronic mobility of graphene, which previously has only been done within the model of idealized Coulomb scatterers, but not within a fully quantum mechanical scattering approach. We find good agreement with experiments in the case of Au and Pt adatoms. We also give predictions for the cases of hydrogen and vacancy scattering. We find that the detrimental effect on the mobility is notably smaller for Pt and H than for Au and vacancies. We also find that screening proves to be a crucial factor when calculating impurity-limited electronic mobilities. The overall magnitude of the impurity results, which are significantly smaller than the phonon-limit, shows that extrinsic effects should typically dominate conduction in graphene, it also shows that it is indispensible to have a theory such at the present AIM approach that allows the introduction of scattering from impurities that are present in the environment; this provides a much more realistic comparison with available experiments. Our present study has thus shown that the AIM approach gives reasonable *ab-initio*

predictions for electron mobilities, which provides unique opportunities for exploratory work to computationally discover and design new 2D materials with desired properties.

Acknowledgments

This research was funded by the Center for Emergent Materials at The Ohio State University, an NSF MRSEC (Grant No. DMR-0820414). We also thank the Ohio Supercomputer Center for support under Project Nos. PAS0072 and PAA0010.

Chapter 3: Electronic Mobilities in WS_2 and WSe_2 from *Ab-initio* calculations

Abstract

The electronic and hole mobilities for two-dimensional transition metal dichalcogenides WS_2 and WSe_2 sheets are calculated completely from first-principles. We predict lattice-scattering limited electron mobilities of 540 and 1424 cm^2/Vs for perfect, suspended WS_2 and WSe_2 respectively, considerably higher than the 200 cm^2/Vs found for the more abundantly studied MoS_2. We also introduce a novel method for the ab-initio calculation of hole mobilities. We report values for the lattice-scattering limited hole mobilities of 116 and 435 cm^2/Vs for WS_2 and WSe_2, respectively.

Introduction

Graphene stands as the two-dimensional (2D) material with the highest mobility to date, reaching 200,000 cm^2/V-s, making it an excellent conductor[43]. However, its lack of a band gap diminishes its usefulness in certain electronic applications. Graphene's large mobility still remains enticing, so a search for other 2D materials with a band gap and a similarly large electron mobility is underway. Among the planar materials receiving scrutiny are the transition metal dichalcogenides (TMDs). TMDs are useful for studying 2D materials because they transition from indirect band gap materials to direct gap materials as their number of layers decreases [44]. This allows for studying the quantum confinement effects that 2D materials experience.

Of the TMDs, MoS_2 has received the greatest attention. Radisavljevic *et al.* produced a monolayer MoS_2 transistor with a mobility of ~200 cm^2/Vs and a large on/off ratio exceeding 10^8 [45]. This mobility matches roughly that of graphene nanoribbons, leading to MoS_2 to be an appealing material in optoelectronics, since it is not only thin but also has a respectable mobility [46]. In this study, we examine the electron and hole mobilities of single layer WS_2 and WSe_2 with first-principles modeling. The tungsten TMDs have heavier atoms than MoS_2 which leads to the expectation that they should have a larger electron mobility, with WSe_2 being the heavier of the two tungsten TMD[47]. Furthermore, it is expected that the band gap of the WSe_2 should be smaller than that of WS_2 since the band gap should decrease as the chalcogenide (i.e. S, Se) atomic number increases[63]. Zhao *et al.* found that WS_2 and WSe_2 have potential as "tailored optoelectric, eletrocatalytic, and photocatalytic functionalities", and emitted 20-40 times intense light

than MoS_2[48]. In fact, WSe_2 has been made into a 2D p-n junction with a strong photodiode capability[49]. WS_2 and WSe_2 have been used for transistors with a promising on/off ratio of 10^5-10^6 and 10^6 [50,51]. WS_2 and WSe_2 can be produced through the sulfurization and selenization of WO_3, respectively[52,53]. Furthermore, WS_2 and WSe_2 have also been mechanically exfoliated from their bulk structures[6,7] .

We use first principles to determine the electron and hole mobility of WSe_2 and WS_2 as a function of temperature. The band structure was also used to determine the effective charge carrier masses at the band gap. We obtain the electron-phonon scattering rates as a function of energy. We find that mobility of WSe_2 and WS_2 are significantly greater than the mobility for MoS_2. We also find the band gap shows that these two tungsten TMDs are direct gap and possess band gaps the size of MoS_2 or larger.

Methods

The positions of the atoms in the unit cell for both WS_2 and WSe_2 systems were relaxed using VASP[54,55]. Then the HSE06 exchange-correlation functional was used through VASP to calculate their band structures[56]. The mobility calculations performed with the Quantum ESPRESSO software suite, which uses local density approximation to follow the density functional perturbation theory calculations established by Restrepo *et al*[47]. The mobility calculations will be limited to room temperature phonon-electron interactions to find the theoretical ultimate limit for the mobilities. Additionally, these calculations assume flat, unstrained, suspended sheets in vacuum because the mobility is sensitive to strain and substrate effects.

We also introduce a method to calculate hole mobilities from first-principles. We use the following formulas:

The hole mobility is calculated using:

$$\mu = -\frac{2h}{n_c}\sum_j \int_0^{-k_F} \frac{d^3\vec{k}}{(2\pi)^3}\tau(\vec{k}j)\vec{v}_j^2(\vec{k})\frac{df}{d\varepsilon}\Big|_{\varepsilon=\varepsilon(\vec{k}j)} \quad (5)$$

Where n_c is the density of charge carriers, $v_j(k)$ are the electronics velocities, $\tau(k)$ is the scattering rate, and f is the Fermi-Dirac distribution. The scattering time is described as:

$$\frac{1}{\tau} = \frac{2\pi}{\hbar}\sum_{\vec{q}hj'} \left|g^{\vec{q}\lambda}_{\vec{k}+\vec{q}j',kj}\right|^2 \times \left\{\left[1 - f\left(\varepsilon_{\vec{k}+\vec{q}j'}\right) + n_{\vec{q}\lambda}\right]\delta\left(\varepsilon_{\vec{k}j'} - \varepsilon_{\vec{k}+\vec{q}j'} + \hbar\omega_{\vec{q}\lambda}\right) + \left[n_{\vec{q}\lambda} - f(\varepsilon_{\vec{k}+\vec{q}j'})\right]\delta\left(\varepsilon_{\vec{k}j'} - \varepsilon_{\vec{k}+\vec{q}j'} - \hbar\omega_{\vec{q}\lambda}\right)\right\} \quad (6)$$

Where $\varepsilon_{\vec{k}j'}$ are energy bands, $\omega_{\vec{q}\lambda}$ are the phonon energies, $n_{\vec{q}\lambda}$ is the Bose- Einstein distribution function, $f\left(\varepsilon_{\vec{k}+\vec{q}j'}\right)$are Fermi-Dirac occupation factors, and g is the e-p coupling function.

Results and Discussion

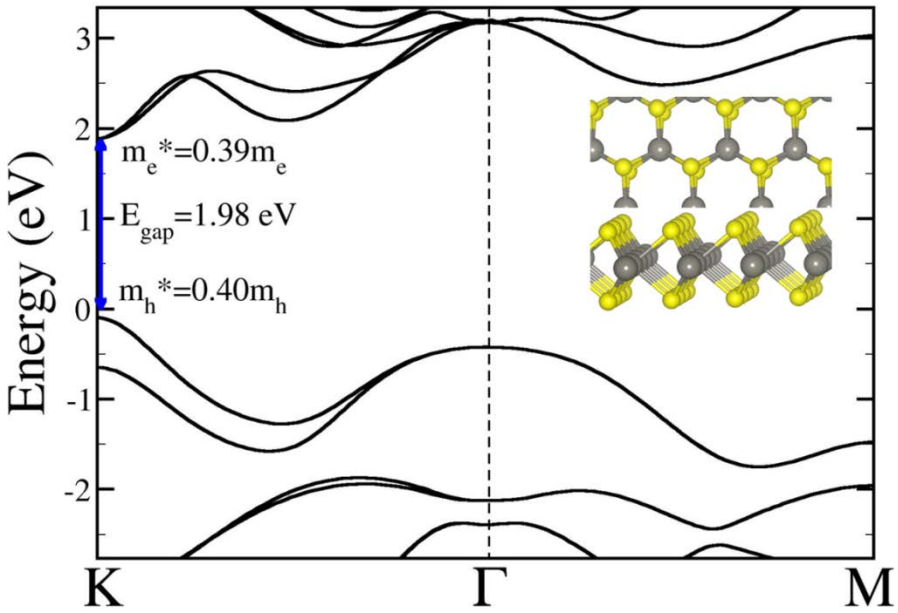

Figure 10: WS_2 Band Structure from HSE Calculations

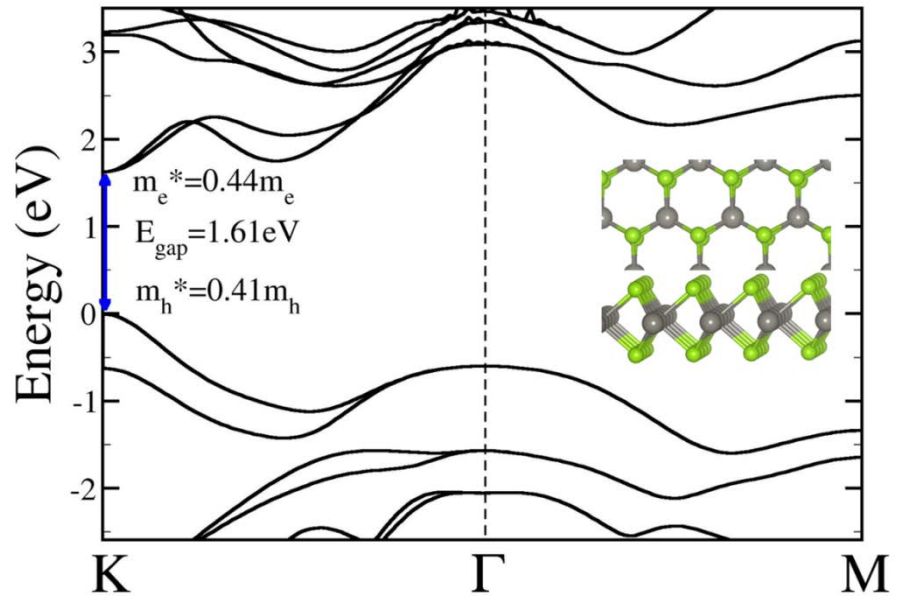

Figure 11: WSe_2 Band Structure from HSE Calculations

The band structures of WS_2 and WSe_2 calculated using HSE are shown in Figures 10 and 11. The calculated band gap and effective masses of electrons and holes along with the predicted room-temperature mobilties of WS_2 and WSe_2 are listed in Table II. Shi *et al.*, [57] suggests that these band gap values are for the optical band gap, not the electronic gap. The calculations are consistent with our earlier prediction that the band gap of WSe_2 should be smaller than that of WS_2.

Table II: Band Gap, Effective Masses, and Phonon-limited Mobilities at 300 K for WS_2 and WSe_2

	Band Gap (eV)		**Effective Mass (m*/m)**		**Mobility (cm^2/Vs)**			
	Calculated	Others	Electrons	Holes	Electron	Experiment	Holes	Experiment
WS_2	1.96	2.14[50]	0.39	0.40	540	44[50]	116	43[50]
WSe_2	1.61	1.6[62]	0.44	0.41	1424	142[62]	435	250[51]

At room temperature, WSe_2 has a phonon-limited electron(hole) mobility of 1424 (435) cm^2/Vs. WS_2 has a phonon-limited electron(hole) mobility of 540 (116) cm^2/Vs. As shown in Table I, these electron mobilities far exceed experimental results. The lower experimental mobilities may be attributed to substrate, strain, or doping effects. Previously, we have obtained good experimental agreement for silicon, graphene,

graphene, and monolayer MoS_2[5, 17], this gives us confidence that these results predict an idealized case when the only scattering comes from electron-phonon interactions. The most notable prediction is that the mobility of WS_2 and WSe_2 is roughly 2 and 4 times greater than that of MoS_2's predicted mobility of 225 cm^2/Vs[58]. Compared to prediction by Jin *et al.*, these room temperature mobilities are significantly greater[59]. The effective electron (hole) masses of WS_2 and WSe2 are 0.39 (0.4) and 0.44 (0.41), respectively, while the electronic mass of MoS_2 is 0.5 which is consistent with a lower mobility.

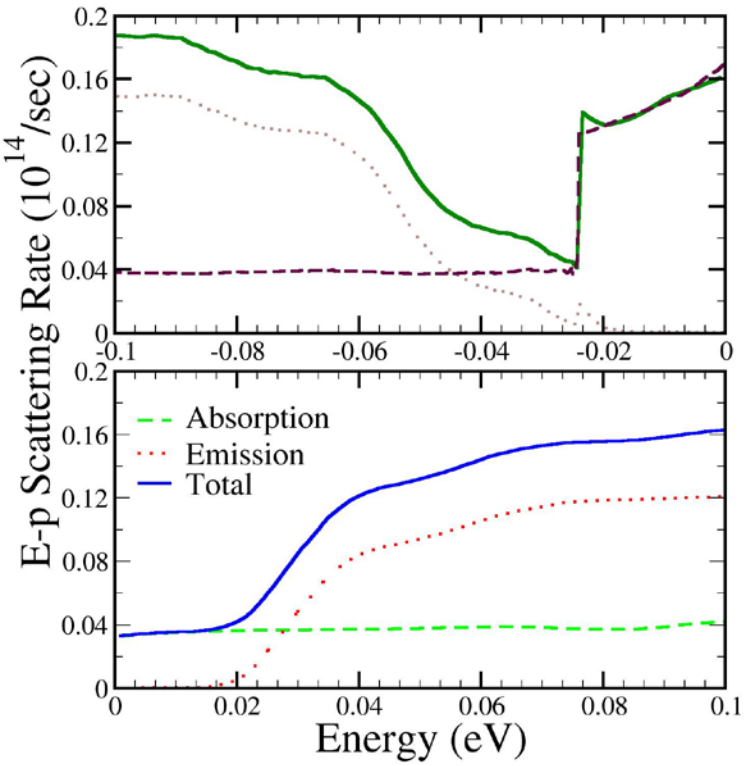

Figure 12: Hole (top) and Electron (bottom) Scattering Rates for WS_2

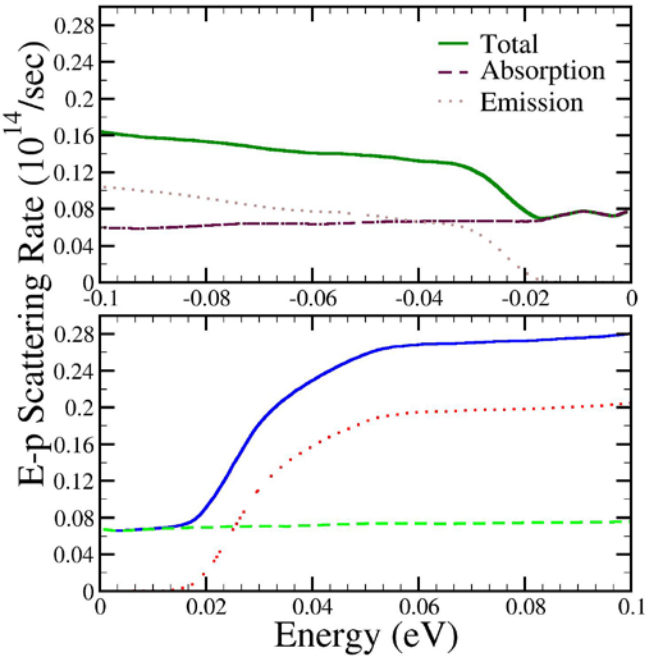

Figure 13: Hole (top) and Electron (bottom) Scattering Rates for WSe_2

Figures 12 and 13 show the electron and hole scattering rates for both WS_2 and WSe_2. The appearances of the scattering rate of both tungsten dichalcogenides follows the expected behavior of the emission scattering overwhelming the absorption scattering [Jacoboni Fig. 9.4][60]. The early stages, before 0.02 eV, show the absorption scattering, but then the emission scattering dominates. The discontinuity of the WS_2 hole scattering rate is caused by the close energy level of the local maxima at the Γ and K points, which sharply increases the density of states, and in turn, sharply decreases the scattering rate.

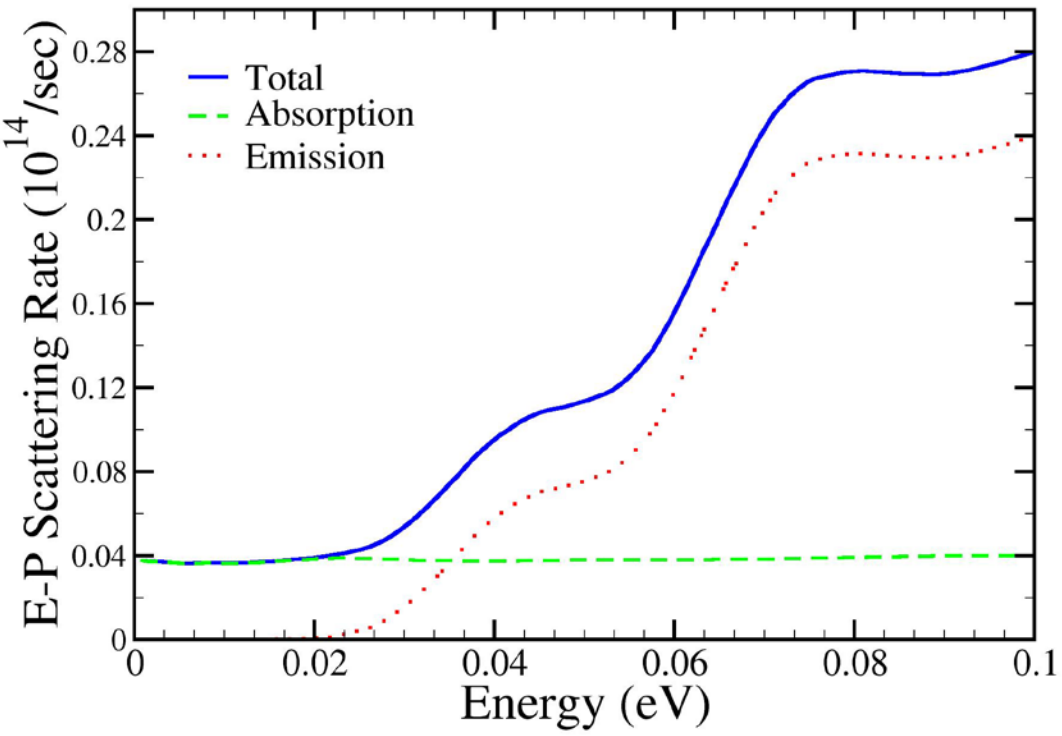

Figure 14: Electron Scattering Rate for MoS_2

In comparing these scattering rates to that of MoS_2, shown in Figure 14, the scattering rate of the tungsten TMDs is greater than that of MoS_2. By this metric, the electron mobility of MoS_2 should be greater than that of WS_2 and WSe_2. According to the mobility equation (equation 1) described in [47], the two major contributors to mobility should be the scattering rate and electron velocity. By giving the MoS_2 and WSe_2 the velocities of the other, one finds that they would then have electron mobilities of 2153 and 86 cm^2/Vs respectively. This dramatic reversal shows that the velocity is responsible

for the large mobility of WSe_2 over MoS_2. Although the scattering rate for WS_2 is greater than for MoS_2 at room temperature, the difference in effective masses plays a significant factor in WS_2's greater mobility as well.

The temperature dependent mobility for both dichalcogenides is shown in Figure 15 and 16. Comparing to the experimental results published by Chuang *et al.*, the calculated mobilities at ~75 and ~150 K are orders of magnitude greater, suggesting that the phonon-limited mobility at these temperatures may be much greater than found experimentally to date[61]. For the WS_2, the electron and hole temperature dependence follows a temperature dependence of T^{-4} and $T^{-3.7}$ respectively. The WSe_2 has an electron and hole temperature dependence of $T^{-3.8}$ and $T^{-4.2}$.

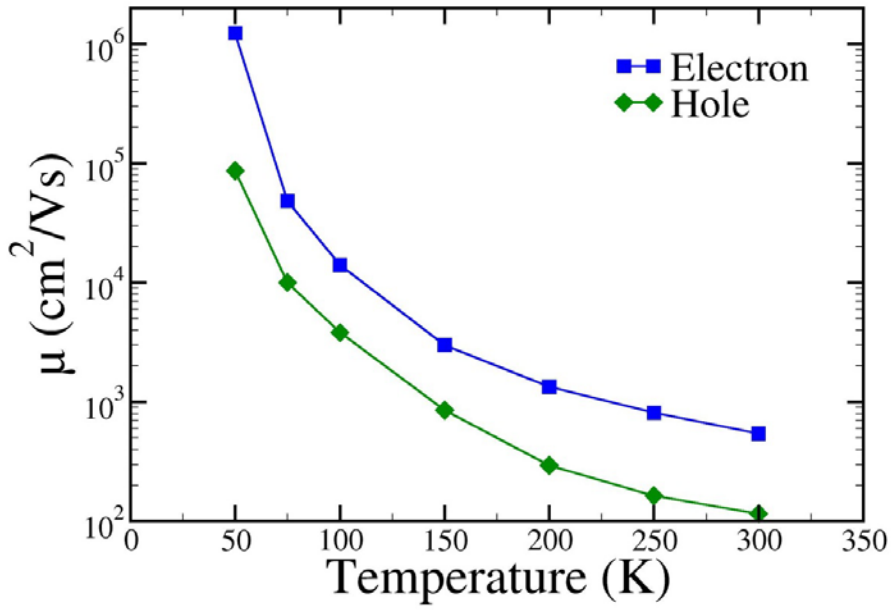

Figure 15: WS_2 Temperature Dependent Mobilties for Holes and Electrons

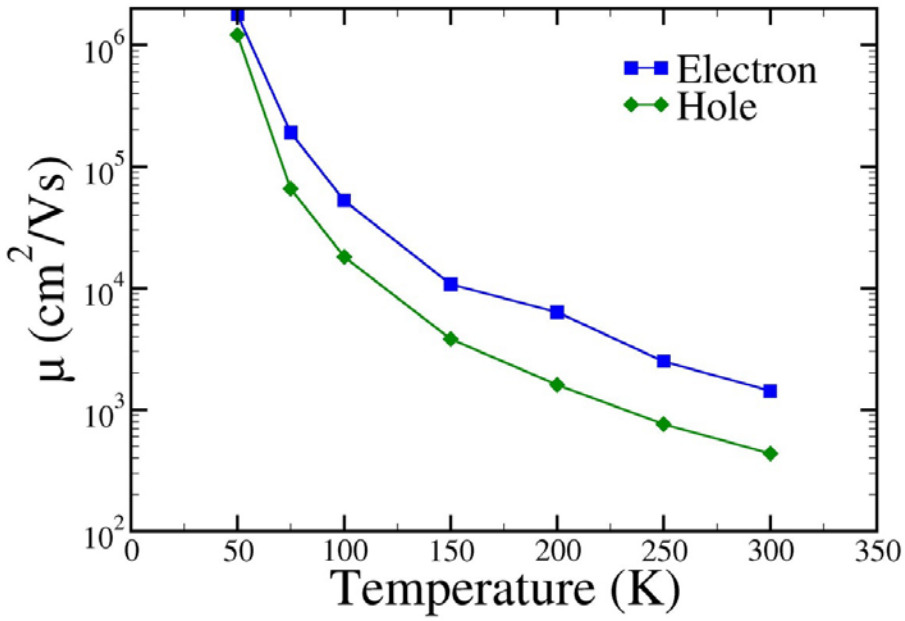

Figure 16: WSe_2 Temperature Dependent Mobilities for Holes and Electrons

Conclusions

First principles calculations were used to determine the electron mobilties of WS_2 and WSe_2. It was found that the phonon-limited mobility of WS_2 was 540 cm^2/Vs and for WSe_2, it was 1424 cm^2/Vs. The hole mobility was determined by using modified and developed equations. The hole mobilities of WS_2 and WSe_2 were found to be 116 and 435 cm^2/Vs respectively. WS_2 and WSe_2 show great potential based on these calculations due to their electronic velocities, which is enough to overcome the smaller scattering rate of MoS_2. In terms of mobility and band structure, it is predicted that WS_2 outclasses MoS_2 with little compromise in the band structure. WSe_2 is close to meeting

the criteria for a high-efficiency single junction photovoltaic, according to the Shockley-Quessier limit[62].

Acknowledgements

This research was funded by the Center for Emergent Materials at The Ohio State University, an NSF MRSEC (Grant No. DMR-0820414). We also thank the Ohio Supercomputer Center for support under Project No. PAS0072. We would also like to thank the Ohio Stem Ability Alliance for their support.

Chapter 4: Conclusions

By using the calculation methods devised by Restrepo *et al.*, good agreement is found with experimental electron mobility results of the well-studied graphene, graphene, and monolayer and bulk MoS_2 systems. After establishing the reliability of these predictions, we then predicted the electron mobility of the tungsten transition metal dichalcogenides, WS_2 and WSe_2. Furthermore, we developed a method to calculate the hole mobility of 2D materials. While current experimental results do not agree with the electronic mobility of these materials, the agreement with experiment on previous 2D materials suggests that the predicted results are reliable. Furthermore, an investigation of the scattering rates and band structures reveal no anomalies. These results also follow expected changes in that the heavier atoms should have larger electron mobilities due to their larger masses and that the chalcogen cation determines the size of the band gap. As far as predictions go, WS_2 and WSe_2 have potential to surpass MoS_2 in terms of utility. Both possess a greater mobility than MoS_2 due to their electronic velocities despite MoS_2's lower scattering rate and WSe_2's electron mobility is cause for excitement and requires further investigation.

References

([1]) A.K. Geim and K. S. Novoselov: The Rise of Graphene. *Nat. Mat.*, **6**, 183-191, (2007).

([2]) S. Z. Butler *et al.*: Progress, Challenges, and Opportunities in Two-Dimensional Materials Beyond Graphene. *ACS Nano* **7**(4), 2898-2926 (2013).

([3]) S. Das Sarma, S. Adam, E. H. Hwang, E. Rossi: Electronic transport in two-dimensional graphene. *Rev. Mod. Phys*. **83**, April-June (2011).

([4]) E. Bianco, S. Butler, S. Jiang, Y-H Liu, O. D. Restrepo, W. Windl, J. E. Goldberger: Hydrogen-terminated germanane; An air-stable germanium graphane analogue. *ACS Nano,* **7**(5), 4414-4421 (2013).

([5]) T. Ando, A. B. Fowler, and F. Stern, Rev. Mod. Phys. **54**, 437 _1982_.

([6]) M. Fischetti and S. E. Laux, Phys. Rev. B **48**, 2244 _1993_.

([7]) B. K. Ridley, Quantum Processes in Semiconductors, 4th ed. (Oxford University Press Inc., New York, 1999).

([8]) C. Herring and E. Vogt, Phys. Rev. **101**, 944 _1956_.

([9]) C. Jacoboni and L. Reggiani, Rev. Mod. Phys. **55**, 645 _1983_.

([10]) A. Abramo, L. Baudry, R. Brunetti, R. Castagne, M. Charef, F. Dessenne, P. Dollfus, R. Dutton, W. L. Engl, R. Fauquembergue, C. Fiegna, M. V. Fischetti, S. Galdin, N. Goldsman, M. Hackel, C. Hamaguchi, K. Hess, K. Hennacy, P. Hesto, J. M. Higman, T. Iizuka, C. Jungemann, Y. Kamakura, H. Kosina, T. Kunikiyo, S. E. Laux, H. Lin, C. Maziar, H. Mizuno, H. J. Peifer, S. Ramaswamy, N. Sano, P. G. Scrobohaci, S. Selberherr, M. Takenaka, T.-W. Tang, K. Taniguchi, J. L. Thobel, R. Thoma, K. Tomizawa, M. Tomizawa, T. Vogelsang, S.-L. Wang, X. Wang, C. Yao, P. D. Yoder, and A. Yoshii, IEEE Trans. Electron Devices **41**, 1646 _1994_.

([11]) V. Kotov, J. Stiens, and G. Shkerdin, J. Appl. Phys. **91**, 3992 _2002_.

([12]) H. Peelaers and C. G. Van de Walle: Effects of strain on band structure and effective masses in MoS_2. *Phys. Rev. B* **86**, 241401(R) (2012).

([13]) O. D. Restrepo, K. Varga, S. T. Pantelides: First Principles Calculations of Electron Mobilities in Silicon: Phonon and Coulomb Scattering. *Appl.Phys.Lett.* **94**, 212103 (2009).

([14]) S. Baroni et al., QUANTUM ESPRESSO, http://www.pwscf.org/, 2010.

([15]) W. Kohn and L. Sham: Self-Consistent Equations Including Exchange and Correlation Effects. *Phys. Rev.* **140**, A1133-A1138 (1965).

([16]) G. Mahan, *Many-Particle Physics*, 3rd ed. _Plenum, New York, 2000.

([17]) S. Baroni, S. de Gironcoli, A. Dal Corso, and P. Giannozzi: Phonons and related crystal properties from density-functional perturbation theory. *Rev. Mod. Phys*. **73**, 515 (2001).

([18]) P. E. Blöchl, O. Jepsen, and O. K. Andersen: Improved tetrahedron method for Brillouin Zone integrations. Phys. Rev. B **49**, 16223 (1994).

([19]) O. D. Restrepo and W. Windl: Full first-principles theory of spin relaxation in group-IV materials. *Phys. Rev. Lett.* **109**(16), 166604 (2012).

([20]) J. Pernot, C. Tavares, E. Gheeraert, E. Bustarret, M. Katagiri, and S. Koizumi: Hall electron mobility in diamond. *Appl. Phys. Lett.* 89, 122111 (2006).

([21]) K. Kaasbjerg, K. S. Thygesen, and K. W. Jacobsen: Phonon-limited mobility in n-type single-layer MoS_2 from first-principles. *Phys. Rev. B* **85**, 115317 (2012).

([22]) Jorge O. Sofo *et al.*: Graphane: A two-dimensional hydrocarbon. *Phys. Rev. B.* **75**, 153401 (2007).

([23]) S. Lebegue, M. Klintenberg, O. Eriksson, and M. I. Katsnelson: Accurate electronic band gap of pure and functionalized graphane from GW calculations. *Phys. Rev. B* **79**, 245117 (2009).

([24]) X. Du, I. Skachko, A. Barker, and E. Y. Andrei: Approaching ballistic transport in suspended graphene. *Nature Nanotech*. **3**, 491-495 (2008).

([25]) K. I. Bolotin, K. J. Sikes, Z. Jiang, M. Klima, G. Fudenberg, J. Hone, P. Kim, and H. L. Stormer: Ultrahigh electron mobility in suspended graphene. *Solid State Commun.* **146**, 351-355 (2008).

([26]) E. Tiras, S. Ardali, T. Tiras, E. Arslan, S. Cakmakyapan, O. Kazar, J. Hassan, E. Janzén, and E. Ozbay, Effective mass of electron in monolayer graphene: Electron-phonon interaction , *J. Appl. Phys*. **113**, 043708 (2013).

([27]) J. P. Perdew, K. Burke, and M. Ernzerhof: Generalized gradient approximation made simple. *Phys. Rev. Lett*. 77, 3865-68 (1996).

([28]) Y. Wang, X. Xu, J. Lu, M. Lin, Q. Bao, B. Ozyilmaz, and K. P. Loh: Toward High Throughput Interconvertible Graphane-to-Graphene Growth and Patterning. *ACS Nano*. **4**. 6146-6152. 2010

([29]) K. M. McCreary, K. Pi, A. G. Swartz, W. Han, W. Bao, C. N. Lau, F. Guinea, M . I. Katsnelson, R. K. Kawakami: Effect of cluster formation on graphene mobility. *Phys. Rev. B* **81**, 115453 (2010).

([30]) K. Pi, K. M. McCreary, W. Bao, W. Han, Y. F. Chiang, Y. Li, S.-W. Tsai, C. N. Lau, and R. K. Kawakami: Electronic doping and scattering by transition metals on graphene. *Phys. Rev. B* **80**, 075406 (2009).

([31]) B. Radisavljevic, A. Radenovic, J. Brivio, V. Giacometti, and A. Kis: Single-layer MoS_2 transistors. *Nat. Nano.* **6**, 147 (2011).

([32]) H. Peelaers and C. G. Van de Walle: Effects of strain on band structure and effective masses in MoS_2. *Phys. Rev. B* **86**, 241401(R) (2012).

([33]) K. S. Novoselov, D. Jiang, F. Schedin, T. J. Booth, V. V. Khotkevich, S. V. Morozov, and A. K. Geim: Two-dimensional atomic crystals. *Proc. Natl Acad. Sci*. USA **102**, 10451–10453 (2005).

([34]) A. Ayari, E. Cobas, O. Ogundadegbe, and M. S. Fuhrer: Realization and electrical characterization of ultrathin crystals of layered transition-metal dichaclcogenides. *J. Appl. Phys.* **101**, 014507 (2007).

([35]) Fivaz and E. Mooser: Mobility of charge carriers in semiconducting layer structures. *Phys. Rev.* **163**, 743 (1967).

([36]) X. Li, J. T. Mullen, Z. Jin, K. M. Borysenko, M. B. Nardelli, and K. W. Kim: Intrinsic electrical transport properties of monolayer silicene and MoS_2 from first principles. *Phys. Rev. B* **87**, 115418 (2013).

([37]) K. Kaasbierg, K. S. Thygesen, and K. W. Jacobsen: Phonon-limited mobility in n-type single-layer MoS_2 from first-principles, Phys. Rev. B **85**, 115317 (2012).

([38]) H. Wang, L. Yu, Y-H Lee, Y. Shi, A. Hsu, M. L. Chin, L-J Li, M. Dubey, J. Kong, and T. Palacios: Integrate Circuits Based on Bilayer MoS_2 Transistors. *Nano. Lett.* **12.** 4674-4680, 2012.

([39]) S. Jiang, S. Butler, E. Bianco, O. D. Restrepo, W. Windl, and J. E. Goldberger, *Improving the stability and optical properties of germanane via one-step covalent methyl-termination,* Nat. Commun. 5,3389 (2014).

([40]) J. Heyd, G. E. Scuseria, M. Ernzerhof: Hybrid functionals based on a screened Coulomb potential. *J. Chem. Phys.* **118**, 8207-15 (2003).

([41]) J. Heyd, G. E. Scuseria, M. Ernzerhof: Hybrid functional based on a screened Coulomb potential (vol **118**, pg 8207, 2003) *J. Chem. Phys.*, 124 (2006).

([42]) J. Paier, M. Marsman, K. Hummer, G. Kresse, I. C. Gerber, J. G. Angyan: Screened hybrid density functional applied to solids (vol **124**, pg 154709 2006) *J. Chem. Phys.*, 125 (2006).

([43]) S.V. Morozov, *et al.*, "Giant Intrinsic Carrier Mobilities in Graphene and Its Bilayer," *Phys Rev Lett.* **100**, 016602, (2008)

([44]) Kumar, A., *et al,;* "Electronic structure of transition metal dichalcogenides monolayers 1H-MX_2 (M = Mo, W; X= S, Se, Te) from ab-initio theory: new direct band gap semiconductors." *The European Physical Journal B.* **85,** 186, 2012

([45]) Radisavljevic, B., *et al.*; "Single-layer MoS_2 transistors". *Nature Nano.*, **6**, 147-150, (2011)

([46]) Molina-Sánchez, A., *et al.,* "Phonons in single-layer and few-layer MoS_2 and WS_2." *Phys. Rev. B.*, **84,** 155413, (2101)

([47]) Restrepo, O.D., *et al.*; " First-principles calculations of electron mobilities in silicon: Phonon and Coulomb scattering". *App. Phys. Letters.* **94**, 212103 (2009)

([48]) Zhao, Weijie, *et al.;* "Evolution of Electronic Structure in Atomically thin sheets of WS_2 and WSe_2," *ACS Nano.* **7,** 791-797, 2013

([49]) Bratschitsch, Rudolf; "Optoelectronic device: Monolayer diodes light up", *Nat. Nano.* **9**, 247-248, 2014

([50]) Jo, Sanghyun, *et al.*; "Mono- and Bilayer WS_2 Light-Emitting Transistors," *Nano Letters*. **14**, 2019-2025, 2014

([51]) Fang, Hui., *et al.*; "High-Performance Single Layered WSe_2 p-FETs with Chemically Doped Contacts." *Nano Letters*. **12**, 3788- 3792, 2012

([52]) Cong, Chunxiao, *et al.;"* Synthesis and optical properties of large-scale single-crystalline two-dimensional semiconductor WS_2 monolayer from chemical vapor deposition.", *Adv. Opt. Mat.,* 2014

([53]) Huang, Jing-Kai, *et al.* "Large-Area Synthesis of Highly Crystalline WSe_2 Monolayers and Device Applications," *ACS Nano.* **8,** 923-930, 2014

([54]) Kresse, G., Hafner, J.; "*Ab-initio* molecular dynamics simulation of the liquid-metal-amorphous-semiconductor transition in germanium," *Phys Rev B.* **49**. 14251-14269, 1993

([55]) Kresse, G., Hafner, J.; "*Ab-initio* molecular dynamics for liquid metals," *Phys Rev B.* **47**. 558-561, 1993

([56]) Heyd, J., Scuseria, G.E., Ernzerhof, M.; "Hybrid Functionals based on a screened Coulomb potential," *J. Chem. Phys.* **118**, 8207-8215, 2003

([57]) Shi, Hongliang, *et al.*, "Quasiparticle band structures and optical properties of strained monolayer MoS_2 and WS_2." *Phys. Rev. B.*, **87.** 155304 (2013)

([58]) Restrepo, Oscar D., *et al.*; "A first principles to simulate electron mobilities in 2D materials." *New Journal of Physics*. **16**. 2014

([59]) Jin, Zhenghe, *et al.*; " Intrinsic transport properties of electrons and holes in monolayer transition metal-dichalcogenides." *Phys. Rev B.* **90.** 045422. (2014)

([60]) Jacoboni, Carlo. *Theory of Electron Transport in Semiconductors*. Berlin Heidelberg: Springer, 2010, pp. 141

([61]) Chuang, Hsun-Jen, *et al.* " High Mobility WSe_2 p- and n-Type Field-Effect Transistors Contacted by Highly Doped Graphene for Low-Resistance Contacts." *Nano Letters*. **14**. 3594-3601, 2014

([62]) Jariwala, Deep; *et al,;* "Emerging Device Applications for Semiconducting Two-Dimensional Transition Metal Dichalcogenides," *ACS Nano.* **8**, 1102-1120, 2014

([63]) Liu, Wei, *et al.*; "Role of Metal Contacts in Designing High-Performance Monolayer n-type WSe_2 Field Effect Transistors," *Nano Letters*. **13**. 1983-1990, 2013